Available online at www.sciencedirect.com
SCIENCE DIRECT®
Polymer 45 (2004) 101–115
polymer
www.elsevier.com/locate/polymer

Facile synthesis of highly soluble copolymers and sub-micrometer particles from ethylaniline with anisidine and sulfoanisidine

Xin-Gui Li[a,b,c,*], Mei-Rong Huang[a], Wei Feng[a], Mei-Fang Zhu[b], Yan-Mo Chen[b]

[a]*Institute of Materials Chemistry, State Key Laboratory of Concrete Materials Research, College of Materials Science and Engineering, Tongji University, 1239 Siping Road, Shanghai 200092, China*
[b]*The State Key Laboratory for Modification of Chemical Fibers and Polymer Materials, Donghua University, Shanghai 200051, China*
[c]*The Key Laboratory of Molecular Engineering of Polymers, Fudan University, Shanghai 200433, China*

Received 19 September 2003; received in revised form 29 October 2003; accepted 31 October 2003

Abstract

Two series of copolymers were synthesized by an oxidative polymerization of 2-ethylaniline (EA) with 2-anisidine (AS) or 5-sulfonic-2-anisidine (SA) for a detailed comparative study between EA/SA and EA/AS copolymers. The preparation, structure, and properties of the copolymers were systematically studied by FT-IR, high-resolution ^{1}H NMR, UV–vis, elementary analysis, GPC, laser particle size analysis, atomic force microscope, and thermogravimetry. Significant dependences of the yield, molecular weight, solubility, and thermostability of the copolymer particles on the comonomer ratio and oxidant/monomer ratio have been observed. The molecular weight increases continuously with increasing EA content in the two copolymers. Quinoid structures favor on the EA units in EA/AS copolymers with the whole oxidation rate of larger than 0.5 in the molecular chain. Although the EA/AS copolymers exhibit only external doping, the EA/SA copolymers exhibit not only external doping on EA units but also self-doping on SA units. The monomer reactivity increases in the order of EA $\leq$ SA $<$ AS. The size and its distribution of the particles are highly dependent on polymerization time and comonomer ratio. The sub-micrometer particles with the smallest diameter of 120 nm are easily prepared by an in situ EA/SA (70/30) polymerization. A relationship between the particle diameter and macromolecular steric model is founded. A new simple method of preparing sub-micrometer particles of aniline derivative polymers without adscititious stabilizer is established. A possible formation mechanism of the sub-micrometer particles during a non-emulsion EA/SA polymerization is proposed. The polymer particles obtained are completely soluble in many solvents and exhibit a very good film-forming ability. A regular variation of the thermostable characteristics of the copolymers with comonomer ratio is found and a three-step process of the thermal degradation is assigned.

Keywords: Ethylaniline copolymer; Sulfoanisidine polymer; Sub-micrometer particle

1. Introduction

The polymers from aniline (AN) and its derivatives are the electrically conductive polymers studied most widely because of their easy preparation, higher stability, variable electroconductivity [1], and important applications including photovoltaic devices [2], light emitting diodes [3], secondary cells, biosensors, electrochromic materials, and anticorrosion coatings [1]. However, the conductive form of PAN is difficult to be processed because it is both unstable at melt-processing temperatures and insoluble in most organic solvents except for *N*-methyl-2-pyrrolidone (NMP) and dimethyl sulfoxide (DMSO), greatly limiting its further practical application. Several ways have been developed to improve its solubility. Among them, the alkyl, alkoxy, and amino ring-substituted [4–7] and N-substituted [8] PANs have caught great interest because of their much better solubility in many common solvents and relatively easy processing. The most successful approach to produce soluble conductive PAN is to introduce sulfonic groups onto the chains [9–14]. These sulfonated PANs are drawing significant attentions because of their greatly improved processing ability and environmental stability due to the presence of sulfonic group together with somewhat high electronic conductivity of 0.1 S/cm [15]. From a practical

* Corresponding author. Address: Institute of Materials Chemistry, State Key Laboratory of Concrete Materials Research, College of Materials Science and Engineering, Tongji University, 1239 Siping Road, Shanghai 200092, China. Tel.: +86-21-65980524; fax: +86-21-65980530.
E-mail address: lixingui@tongji.edu.cn (X.G. Li).

0032-3861/$ - see front matter © 2003 Elsevier Ltd. All rights reserved.
doi:10.1016/j.polymer.2003.10.085

point of view, the sulfonated PANs are interesting because of their unusual electroactivity, frequent self-doping, characteristic optical property and high stability [16,17]. Epstein and co-worker first reported the sulfonic acid self-doped PAN by reacting PAN emeraldine base with oleum [9]. The sulfonated PAN obtained is soluble in aqueous alkali solution, but it leads to dedoping and becomes an insulator. An oxidative polymerization of 5-sulfonic-2-anisidine (SA) results in a soluble SA homopolymer in water [10,11]. The copolymerization of AN with sulfonated AN (SAN) including disulfonated AN also produces water soluble AN/SAN copolymers [18–22]. The copolymers from SAN with AN derivatives, such as 2-anisidine (AS) and 2-toluidine, are found to be water soluble and their structure and properties were discussed by changing comonomer ratio, solvent and heat treatment temperature [21,23]. Obviously, the sulfonic group on the polymer chains is substantially an internal solubilizer. Another important function of the sulfonic groups on the chains could be acted as an internal stabilizer owing to their interchain electrostatic repulsion, thus leading to an in situ fabrication of the fine particles. However, the vital stabilizing effect of the sulfonic groups for the particles has not been reported to our knowledge.

So far, it seems that an emulsion polymerization is one major method of preparing the nano- and sub-micrometer particles. Unfortunately, the emulsion polymerization system must include a large amount of external stabilizer, emulsifier, and dispersant [24–26], leading a complicated composition and seriously restricting their applications of the particles. A new technique of preparing the particles by the oxidative polymerization in a relatively simple reaction medium without additives has been an important subject.

To understand the internal stabilizing function of sulfonic groups for an in situ formation of the sub-micrometer particles, SA and AS were the first chosen to copolymerize separately with 2-ethylaniline (EA) in the polymerization medium without adscititious stabilizer. A simple procedure for preparing the particles with controllable dimensions down to 120 nm was proposed. A clear relationship between the sulfonic group content and particle size was elaborated. Especially, the two series of copolymer particles, EA/SA and EA/AS, were systematically compared in their polymerization yield, molecular structure, size, solubility, film-forming ability, and thermal stability.

2. Experimental

2-Ethylaniline (EA), 2-anisidine (AS), 5-sulfonic-2-anisidine (SA), ammonium peroxydisulfate, NMP, DMSO, tetrahydrofuran (THF) and other solvents were commercially obtained and used as received.

2.1. The preparation of the fine particles of the copolymers

Copolymer particles were simply prepared by an oxidative polymerization of EA with AS or SA. A representative procedure for the preparation of the EA/AS (50/50) copolymer particles is as follows: To 50 ml of a 1 M HCl solution in a 250 ml glass flask were added 3.09 ml (25 mmol) EA, and 2.83 ml (25 mmol) AS. An oxidant solution was prepared separately by dissolving 5.7 g (25 mmol) ammonium peroxydisulfate [$(NH_4)_2S_2O_8$] in 50 ml of 1 M HCl. Both solutions were cooled to 10 °C. The monomer solution was then stirred and treated with the oxidant solution added dropwise at an adding rate of one drop every three seconds at 10 °C. The reaction mixture was vigorously magneto-stirred for 8 h at 10 °C and followed by the open-circuit potential technique. The open-circuit potential and temperature of the polymerization solution were recorded continuously. After the reaction, the virgin HCl salt particles formed were isolated from the reaction mixture by filtration and washed with an excess of water then acetones to remove the oxidant and oligomers. Half of the salt particles was subsequently neutralized in 0.1 M NH_4OH of 150 ml for 24 h to obtain the emeraldine base, and then washed with excess water. Sometimes the salt and base particles of the copolymers in the corresponding solutions were analyzed directly by laser particle size analyzer (LPSA) and atomic force microscope (AFM) before filtration. Both of the solid powders were left to dry in ambient air for one week. The general copolymerization and nominal molecular structure of the final copolymers are described in Scheme 1.

2.2. Measurements

The copolymerization was followed by the open-circuit potential profile technique, using a saturated calomel electrode (SCE) as reference electrode and a Pt electrode as working electrode. The intrinsic viscosity of the copolymers in NMP was measured at 25 °C with an Ubbelohde viscosimeter. The solubility was evaluated: 5 mg of polymer powder was added to 1 ml of solvent and dispersed thoroughly after swaying intermittently for 24 h at room temperature, and the solubility could be characterized semi-quantitatively. The film-formability was studied with NMP and THF as solvents at the concentration of 2 g copolymers in 10 ml solvent by a solution casting method. The NMP in copolymer solutions on glass with the area of 9×9 cm^2 was evaporated by heat treatment at 170 °C for 12 h, while the THF was very easily evaporated even at room temperature (15 °C) due to its low boiling point (66 °C). The size and its distribution of the particles formed just after polymerization or alkaline treatment were analyzed on Beckman Coulter LS230 Particle Size Analyzer. The images were usually taken in a constant height (deflection) mode by using an SPA-300HV AFM system, Seiko SII Instruments, Japan, with a resolution of 0.2 nm in

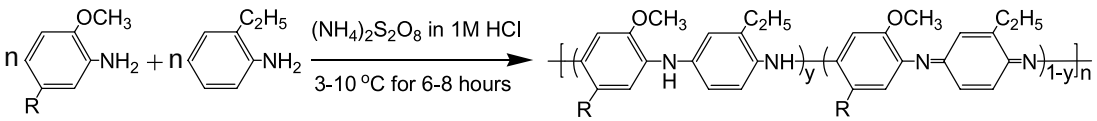

R = SO_3H or H

Scheme 1.

XY direction and 0.01 nm in *Z* direction. The AFM samples were prepared by dropping the dilute aqueous solution of the particles on cover glass, and then drying in air at 25 °C. Elemental analysis was carried out on CE Instrument EA1110 organic element analyzer, Italia. Fluorescence analysis of S and Cl elements was performed on Bruker Axs SRS 3400. IR spectra were recorded on a Nicolet Magna-IR^{TM} 550 spectrometer at 2 cm^{-1} resolutions on KBr pellets. ^{1}H NMR spectra were measured on Bruker DMX 500 at 500.13 MHz at 25 °C. UV–vis absorption spectra were recorded on Perkin Elmer Instruments Lambda 35 at a scanning rate of 480 nm/min. MW and its distribution were measured using HP1100 GPC column (PL-gel mixed C × 2, PL gel 50 nm) and THF as solvent and mobile phase as well as monodisperse polystyrene (MW = 500–10^6 g/mol) as standards. Thermal analysis was performed in a static air with a Perkin Elmer Thermogravimetric Analyzer Pyris 1 TGA at a heating rate of 10 °C/min with the sample size of 4.4–5.6 mg.

3. Results and discussion

3.1. Copolymerization

The oxidative copolymerization is followed by the temperature and potential of the reaction solutions, which may provide a deeper insight into polymerization process. It is found that the oxidative copolymerization of EA and AS monomers is exothermic with the highest temperature rise of 9 °C from the initial temperature 9 °C of the polymerization solution. The solution temperature of all comonomer ratios reaches the maximum value at the maximum potential, indicating the maximal rate point of molecular chain propagation. The maximum potential shows a basically reduced trend from 700 to 640 mV vs SCE as AS content increases from 0 to 100 mol%, and the time corresponding to the maximum and final potentials (t_m and t_f, respectively) shortens from 75 to 17 min and from >110 to 44 min, respectively. It can be ascribed to conjugating and electron-donating effects of $-OCH_3$ with the phenyl ring. This behavior is coincided with the order of the ease of protonation as AN < toluidine < EA < AS reported by Mattoso et al. [27]. This also validates a close relationship between protonation and maximum potential during oxidative polymerization because protonation is the first step of oxidative polymerization.

EA/SA copolymerization exhibits different variation of the solution potential and temperature with reaction time. The maximum potential value remains approximately constant at 710 mV vs SCE as SA feed content increases from 10 to 100 mol%. The maximum potential that has no relations to SA feed content is associated to a thermodynamic factor, which indicates that the initiation of polymerization is mainly caused by EA monomer. With increasing SA content from 10 to 70 mol%, t_m dramatically increases from 80 to >370 min, whereas t_f cannot reach equilibrium during the whole polymerization of 370 min. Since the kinetic factor associates with the time t_m (of propagation) and t_f (of total polymerization), the longer t_m and t_f indicate more difficulty for the monomers to propagate with adding SA unit due to the electron withdrawing and great steric effects of sulfonic acid group on phenyl ring as SA units increase. Note that the potential and time needed for the homopolymerization of three monomers rank in a reduced order.

SA (710 mV and > 370 min) > EA (700 mV and 70 min)

> AS (620 mV and 17 min)

That is to say, the homopolymerizing ability of three monomers ranks in an increased order: SA < EA < AS. Important copolymerization data of EA/AS and EA/SA copolymers are summarized in Tables 1 and 2, respectively. Note that solid EA/SA copolymers with SA feed content of 90 and 100 mol% could not be obtained by a simple filtration or centrifugal separation because of very fine particles formed in situ during their polymerizations, as discussed later. Therefore, the polymers with the EA/SA feed molar ratio of 10/90 and 0/100 could not be listed in Table 2. As shown in the two tables, two series of copolymers both exhibit a maximum yield with the variation of comonomer ratio. However, the maximum yield corresponds to different comonomer ratios, i.e. at EA feed content of 10 mol% for EA/AS copolymer, and at EA feed content of 90 mol% for EA/SA copolymer. A careful comparison of the yield listed in Tables 1 and 2 could educe an order of the monomer ability of forming a polymer: SA ≤ EA < AS. This order is substantially coincided with the analytical result of the solution potential, as discussed earlier. A basically similar variation of the yield with increasing sulfonated AN content was found for AN, AS, and toluidine with sulfonated AN copolymers, respectively [21,28]. The yield of the EA/SA copolymers is also close to that of other sulfonated AN copolymers [18–21]. It should be noticed that two series of copolymers both exhibit the

Table 1
Polymerization data and properties of EA/AS copolymer bases obtained in 1 M HCl aqueous solution with $(NH_4)_2S_2O_8$ as oxidant

EA/AS feed molar ratio	Oxidant/monomer molar ratio	Polymn. temp. (°C)	Polymn. yield (%)	Solubility in NMP (g/L)	Intrinsic viscosity (dL/g)	$\bar{M}_n$ (g/mol)	$\bar{M}_w$	$\bar{M}_w/\bar{M}_n$
100/0	1/2	10	17.4	8	0.28	5620	15,090	2.68
90/10	1/2	10	20.2	6	0.33	5470	7920	1.45
70/30	1/2	10	24.9	8	0.41	4100	5300	1.29
50/50	1/2	10	22.6	6	0.18	3760	4990	1.33
30/70	1/2	10	26.7	5	0.23	4040	5570	1.38
10/90	1/2	10	34.0	5	0.32	[a]	[a]	[a]
0/100	1/2	10	32.8	6	0.29	[a]	[a]	[a]
30/70	1/3	8	17.2	4	[a]	3270	4810	1.47
30/70	1/2	10	26.7	5	0.23	4040	5570	1.38
30/70	3/4	6	45.5	8	0.18	2960	4370	1.47
30/70	1/1	6	68.5	8	0.14	2270	3990	1.76
30/70	5/4	6	72.0	8	0.14	2120	3670	1.73
30/70	3/2	6	61.7	8	0.10	1890	3070	1.63

[a] The MWs or intrinsic viscosity were not measured because the samples are not completely soluble in THF or NMP.

maximum yield at a certain comonomer ratio, indicating that EA and AS or SA are activated each other at least at the initiation stage, i.e. a significant copolymerization effect between EA and AS or SA monomers. The mutual activation between EA and AS or SA monomers results in higher copolymerization yield than respective homopolymerization yields, possibly due to the formation of more activated centers by the copolymerization effect, just like the results caused by increasing oxidant content.

Increasing oxidant/monomer ratio produces higher yield, because greater oxidant/monomer ratio provides more initiatives in the polymerization system. Same relationship between the yield and oxidant/monomer ratio was found for the AN/*m*-sulfonated AN copolymer [28]. Oxidant species have great effects on the copolymerization. For the EA/AS (30/70) copolymerization at the same oxidant/monomer molar ratio of 3/4 at 6–10 °C, the yield steadily increases from 6.9, 21.9, 37.8, 42.9, to 45.5%, as the oxidant changes from $FeCl_3$, $FeCl_3/H_2O_2$(1/10 molar ratio), $K_2S_2O_8$, $Na_2S_2O_8$, to $(NH_4)_2S_2O_8$. This suggests that $(NH_4)_2S_2O_8$ could be the best oxidant for the copolymerization system.

A comparison of the feed and observed comonomer ratios in the copolymers of EA with SA or AS is listed in Table 2. From elementary analysis, it is found that the SA content in the copolymers is always significantly higher than the SA feed content. For the EA/AS copolymers, the observed AS content based on the ^{1}H NMR spectra discussed later is also higher than the corresponding AS feed content. A similar higher content of sulfonic group-containing unit than correspondent feed content was found for AN/*o*-aminophenoxy-*n*-propyl (or *n*-butyl) sulfonic acid copolymers at a low yield of 5–26% [28]. These results indicate higher copolymerization reactivity of AS and SA than EA. In particular, SA exhibits greater reactivity than EA because SA can be activated by EA monomer and hence SA is easily incorporated into growing chains despite of its lower homopolymerization ability. That is to say, the copolymerization activity in EA/AS and EA/SA comonomer pairs ranks in the order of EA < SA < AS. This phenomenon can also be due to the addition of methoxy group, which has the electron-donating effect that increases their reactivity. However, a study on electrochemically copolymerization of AN and disulfonated AN suggests that the incorporation of sulfonic group into the copolymer is rather low [20], which results from low polymerization activity of disulfonated AN due to great steric hindrance and

Table 2
The polymerization yield and composition of EA/SA copolymer virgin salts and EA/AS copolymer emeraldine bases obtained with $(NH_4)_2S_2O_8$/monomer molar ratio of 1/1 in 1 M HCl for 6 h at 3–5 °C

EA/SA feed molar ratio	Polymn. yield (wt%)	EA/SA experimental		Fluorescence analysis	EA/AS molar ratio	
		^{1}H NMR	Elementary analysis	External doping rate (Cl^-) (mol%)	Feed ratio	^{1}H NMR experimental
100/0	17.4[a]	100/0	100/0	–	100/0	100/0
90/10	59.1	81/19	78/22	57	90/10	85/15
70/30	48.5	67/33	66/34	37	70/30	66/34
50/50	42.1	44/56	40/60	46	50/50	37/63
30/70	25.0	22/78	17/83	11	30/70	25/75

[a] The EA homopolymer was polymerized with $(NH_4)_2S_2O_8$/monomer ratio of 1/2 in 1 M HCl aqueous solution at 10 °C.

strong electron-withdrawing effect from two sulfonic groups on each monomer.

3.2. The size of the EA/SA copolymer particles in water

Generally, external stabilizer is deemed to be indispensable to the formation of sub-micrometer polymer particles. It is reported that the particles with mean size in a range of 15–37 μm were formed for the PAN formed in situ by the oxidative polymerization without the external stabilizer [25,29]. In this study, the particle size of the sulfonic group-free EA/AS copolymers ranges from 4 to 7 μm. Nevertheless, the size of the particles formed will become much smaller if less EA with more sulfonated AN derivatives is oxidatively copolymerized in the reaction medium even without any external stabilizer. The particle size of the virgin salts of the EA/SA copolymers exhibits a significant dependency on the comonomer ratio, as shown in Fig. 1. With increasing feed SA content from 30 to 100 mol%, both mean diameter and its standard deviation of the particles first pass through a maximum at EA/SA (50/50) and then monotonically decrease from 10,600 to 218 nm and from 6800 to 131 nm, respectively, because of a significant increase in the negative sulfonic group content on the surface of polymer chain coil, as shown in Fig. 2. Unlike relatively extended configuration of the copolymers (Fig. 2a–c), the SA homopolymer tends to form a spherical configuration (Fig. 2d), also leading to the formation of smaller particles. Moreover, the sub-micrometer particles with the diameter of 218 nm have existed stably in the HCl aqueous solution for at least 6 months. These all indicate that the SA monomer is very favorable for the preparation and stabilization of smaller and evener particles because of the static repulsion of the sulfonic groups. The possible process of particle formation is: First, the primary particulates form at the onset of phase separation in the homogeneous polymerization. Second, the particulates of similar size spontaneously coalesce with each other in order to reduce their surface area and then surface energy

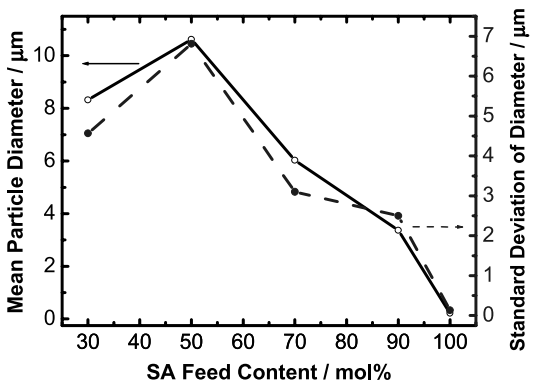

Fig. 1. Variation of particle mean diameter and its distribution of the EA/SA copolymer salts (in water) with SA feed content during the in situ EA/SA copolymerization with ammonium peroxydisulfate as oxidant in 1 M HCl at reaction temperature of 3–5 °C at a constant magneto-stirring rate.

(homocoalescence). Simultaneously, the subsequent growth of the particulates also occurs by absorption of the new particulates formed later (heterocoalescence). In the both cases, the negative bulky sulfonic groups exhibiting static repulsion that were present on the surface of the particulates should migrate to the growing particle surface to help reduce the surface energy and stabilize the particles. Third, both processes proceed until the resultant particles become stabilized due to the static repulsion of the sulfonic groups on the different particles, i.e. when the surface of the particles become mainly covered with enough negative sulfonic groups. The stability and size of the particles depends significantly on the sulfonic group content in the polymer chains. However, not all sulfonic groups may be able to come to the surface. In fact, some may get trapped inside the particles, which may be evidenced by the molecular models in Fig. 2a and b. But with increasing sulfonic groups content, sulfonic groups trapped inside the particles become less and accordingly sulfonic groups on the particle surface become more (Fig. 2c and d). Therefore, the EA/SA polymers with higher SA content of 70–100 mol% exhibit smaller particle diameter than those with lower SA content of 30–50 mol%, as shown in Fig. 1. Particularly, the SA monomer with the highest content of sulfonic groups will give the smallest particles. It is similar to the chemically oxidative synthesis of polypyrrole particles with poly(styrenesulfonates) as template [26]. In addition, note that EA/SA (1/3 and 1/1) copolymers both exhibit an regular and extended helix configuration, which could be valuable for the formation of the materials with anisotropic morphology and properties.

The particle size and its distribution of in situ synthesized EA/SA (30/70, 70/30) copolymer salts were systematically measured and shown in Fig. 3, exhibiting a clear dependency on polymerization time. The EA/SA (30/70) copolymer salts exhibit a very small particle having a mean size of 280 nm and a small standard deviation of the particle diameter of 130 nm at polymerization time of 2 h. Then both the mean size and its standard deviation acutely increase to a maximal value of 6.44 and 3.5 μm, respectively, at 8 h, followed by a declination until to 2.67 and 1.15 μm, respectively, at 24 h. The EA/SA (70/30) copolymer salts exhibit a similar dependency of the particle size and distribution on polymerization time. The difference is that the mean size and its standard deviation of the EA/SA (70/30) copolymer salts appear larger maximal value of 11.4 and 4.7 μm, respectively, at 4 h. Furthermore, the EA/SA (70/30) copolymer salts exhibit larger mean size and its standard deviation during the whole polymerization time than the EA/SA (30/70) copolymer salts. This must be due to higher content of sulfonic group-free EA monomers, bringing on the larger particle size for the EA/SA (70/30) copolymer salts. The variation of the size and its distribution of in situ synthesized particles with the polymerization time indicates an conglomeration of small particles formed earlier and smash of large particles formed later during

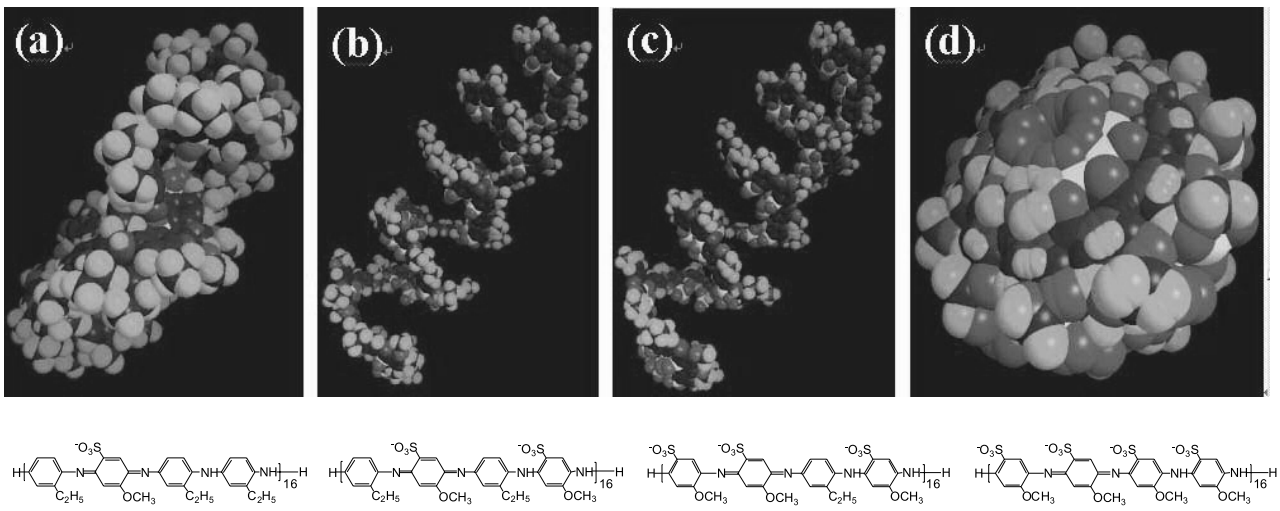

Fig. 2. The macromolecular structure and steric models of a single chain (DP = 64) of (a) EA/SA (3/1) copolymer (MW = 8892); (b) EA/SA (1/1) copolymer (MW = 10,190); (c) EA/SA (1/3) copolymer (MW = 11,502); (d) SA homopolymer (MW = 12,782) with the minimal energy simulated by CS Chem3D Ultra 8.0, CambridgeSoft Corporation, 2003. Yellow, red, green, purple, and sky blue spheres (see web version) represent sulfur, oxygen, nitrogen, carbon, and hydrogen atoms, respectively.

the EA/SA copolymerization. The conglomeration of small particles formed earlier should be a relatively spontaneous process, whereas the smash and uniformization of large particles formed later could be attributed to continual and vigorous stirring magnetically during the polymerization. It is concluded that short polymerization time of about 2 h is benefit to the formation of the very small and uniform particles.

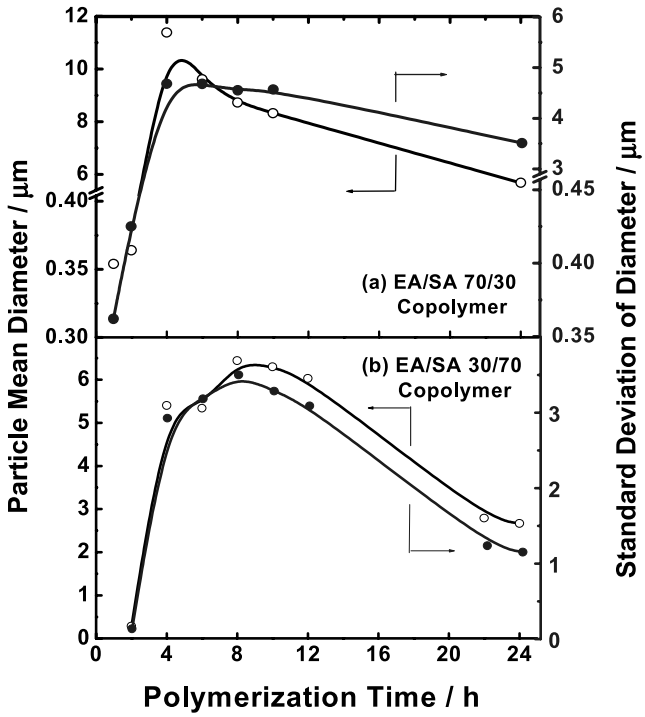

Fig. 3. Variation of the mean diameter and its distribution of the particles (in water) with polymerization time during the copolymerization of EA/SA (a) 70/30 and (b) 30/70 with ammonium peroxydisulfate as oxidant in 1 M HCl at 6–7 °C at a constant magneto-stirring rate.

In addition, upon ammonium treatment, both the mean diameter and its standard deviation of the particles of the EA/SA (50/50) copolymer decrease from 10.6 to 5.6 and from 6.8 to 4.6 μm, respectively, accompanying with a change of the copolymer forms from virgin salt to emeraldine base. This decrease of the particle size could be ascribed to the exclusion of external dopants (HCl) on the copolymer chains.

The size and shape of the polymer particles were further observed by AFM. The particle shape of SA homopolymer virgin salts obtained for the polymerization time of around 6 h seems anomalistic, and their size of about 200 nm is substantially coincided with that (218 nm) found by LPSA. However, with decreasing SA content, the deviation of the particle sizes determined by the two methods becomes great. The particle size of EA/SA (10/90) copolymer salts is around 600 nm that is much smaller than that (3.384 μm) determined by LPSA. Similarly, the size of 120–160 nm of EA/SA (70/30) copolymer salts revealed by AFM in Fig. 4 is much smaller than that (360 nm) by LPSA in Fig. 3a. A close observation of the AFM phase-image in Fig. 4b indicates that the copolymer salt particles of 120–160 nm consist of five or six smaller particulates with the size of 40–70 nm. The smaller particle size observed by AFM than by LPSA must be ascribed to contraction and compression because of the exclusion of water inside the particles during drying. That is to say, AFM samples are equilibrium dry state in ambient air while LPSA samples are swollen by water. Another possible reason is that the AFM results come from two-dimensional projection of image, while the LPSA results are statistically treated by an equivalent sphere model [30]. Moreover, the effect of the contraction and compression becomes stronger with decreasing SA unit content, which is ascribed to a reduced water absorbance from SA units. Similar much smaller particle diameter by

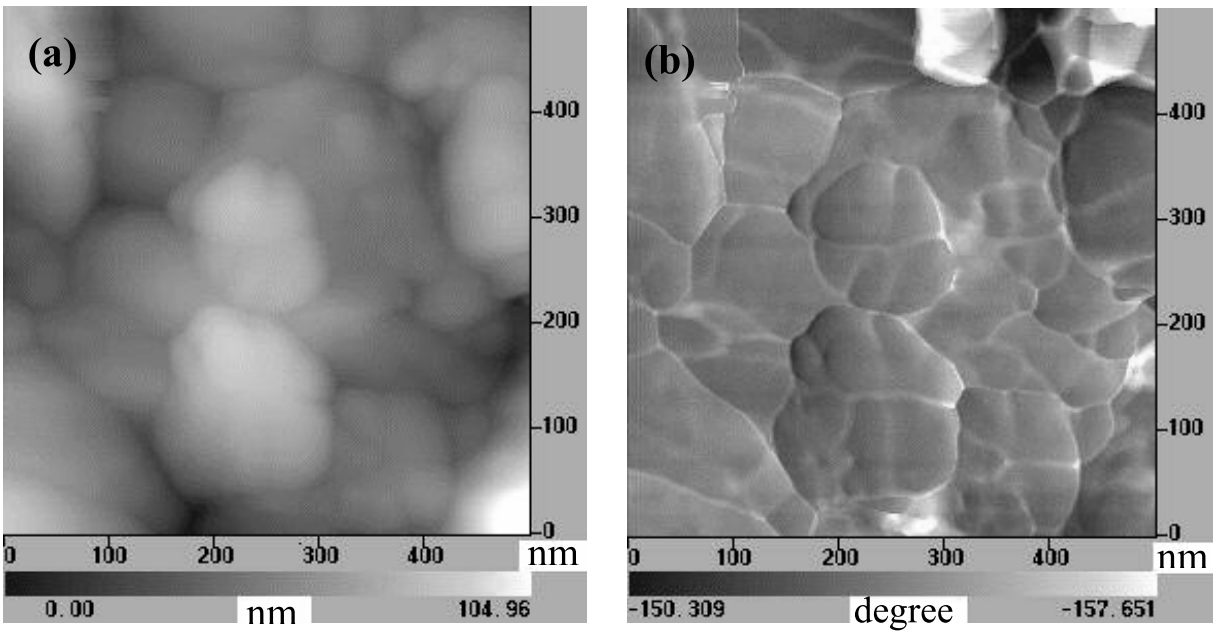

Fig. 4. The typical AFM topoimage (a) and phase-image (b) of EA/SA (70/30) copolymer dry salt particles on a cover glass for the polymerization time of 1 h.

AFM or SEM than by dynamic laser light scattering method has also been observed for highly sulfonated PAN [30] and PPY [31] particles.

In addition, AFM observation also demonstrates a decrease in the particle size after the alkaline treatment. The particle diameter (150–250 nm) of the EA/SA (70/30) copolymer bases obtained by a treatment of NaOH is much smaller than that (5.6 μm in Fig. 3) of the corresponding salt. Similarly, EA/SA (30/70) copolymer base particles after treatment of NaOH and NH_4OH respectively also exhibit much smaller diameter (360 and 380 nm) than that (5.3 μm) of the corresponding salts at 6 h, as shown in Fig. 3b.

It can be concluded that the presence of sulfonic groups on the SA monomers allows the particle size to be controlled by varying the comonomer ratios and polymerization time because the sulfonic groups as an internal stabilizer can produce static repulsion among the particles and further stabilize small particles. Particularly, the particles formed thus are relatively pure because the contamination from the external stabilizer is completely deracinated. The pure particles could be further applied easily and directly for the preparation of nanocomposites, nanocoatings, and transparent electroconducting film with high performance. A new simple method of preparing submicrometer particles of AN derivative polymers by a heterohomogeneous polymerization without any adscititious stabilizer could be inaugurated.

3.3. FT-IR spectra

Representative FT-IR spectra for the EA/SA copolymer salts with SA feed content from 0 to 70 mol% are shown in Fig. 5. The broad band centered at 3385–3454 cm^{-1} is a result of the characteristic free N–H stretching vibration, suggesting the presence of $-NH_2$ and secondary amino groups (–NH–). A shoulder band at 3221 cm^{-1} only for the EA/SA (50/50, 30/70) copolymers is ascribed to the hydrogen-bonded N–H vibration. Three peaks at 2964, 2928 and 2870 cm^{-1} are attributed to C–H stretching vibration in ethyl and methoxy group and steadily become

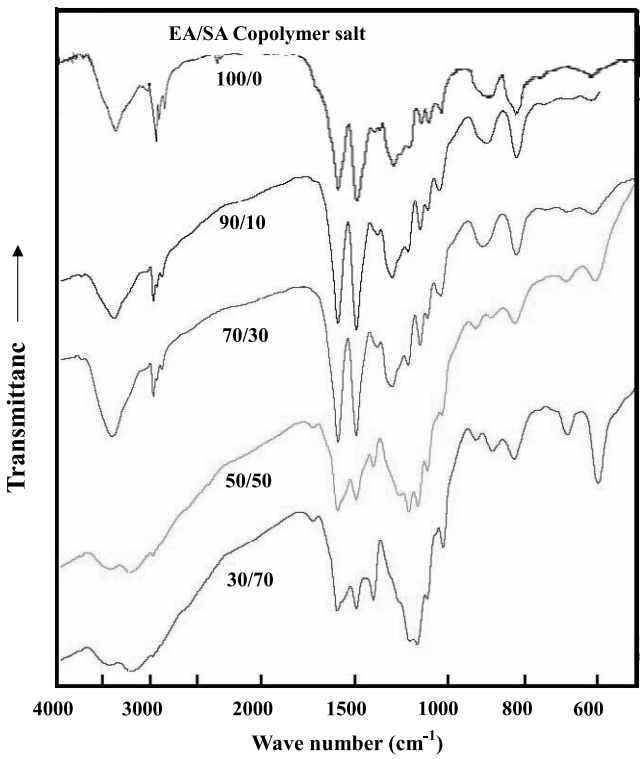

Fig. 5. IR spectra of the copolymer salts with the EA/SA molar ratios of 100/0, 90/10, 70/30, 50/50, and 30/70.

weaker with increasing SA feed content. Two absorptions at 1602 and 1499 cm^{-1} are associated with the stretching of quinoid and benzenoid rings, respectively. As SA content increases from 0 to 70 mol%, an increase in a relative intensity ratio of quinoid to benzenoid structures occurs. If the self-doping takes priority in the SA unit, the external doping favors on EA units and is more thorough than self-doping on SA units. Polymer chain oxidation resulting in a formation of C=O groups may occur in EA/SA (50/50, 30/70) copolymers as suggested by the absorption band at 1736 cm^{-1}. The absorption of copolymers exhibits a steadily increased intensity at 1415, 1214, 1161, 1125, 1028, 685, and 602 cm^{-1} but an almost constant intensity at 884 cm^{-1} as the SA content increases. The strong peaks at 1415 and 685/602 cm^{-1} are ascribed to the stretching vibration of C–S and S–O bonds, respectively. The peaks at 1214 and 1161 cm^{-1} should be due to asymmetric and symmetric O=S=O stretching vibration of SO3 group, respectively, [21]. The absorption at 1028 cm^{-1} is associated with the symmetric stretching of the =C–O–C groups. The band at 1125 cm^{-1} could be only due to the out-of-plane bending vibration of the C–H bond in 1,2,4,5-tetrasubstituted phenyl ring in the SA units. The peak at 884 cm^{-1} due to in-plane bending vibration of the C–H bond in 1,2,4-trisubstituted phenyl ring in the EA units and the out-of-plane bending vibration of the C–H bond in 1,2,4,5-tetrasubstituted phenyl ring in the SA units indicates the formation of the polymers. All the results prove that the EA/SA copolymers have been successfully prepared.

For all of the EA/AS copolymer bases with AS content from 0 to 100%, a broad band centered at 3436 cm^{-1} due to N–H stretching vibration appears, which is similar with those of the EA/SA copolymers. However, with increasing AS content from 0 to 100%, a significant reduction in the relative intensity ratio of quinoid (around 1600 cm^{-1}) to benzenoid (around 1500 cm^{-1}) structures is observed, indicating more favorable of quinoid structure in EA units than in AS units. In particular, the wavenumber difference between quinoid to benzenoid peaks becomes smaller gradually with increasing AS content. These are different from those of the EA/SA copolymers. Weak shoulder peak at 1463–1470 cm^{-1} should be due to the asymmetric bending of $-CH_3$. Similar weak peak at 1384 cm^{-1} attributed to the C–N stretching vibration in quinoid imine units seems the sharpest in the EA homopolymer, proving above result of the favorable quinoid structure on EA units. Two peaks at 1304 and 1248 cm^{-1} could indeed be ascribed to the C–N stretching vibration of quinoid–benzenoid–quinoid alternative and benzenoid–benzenoid–benzenoid block triad sequences, respectively. A remarkable intensity increase in the bands centered at 1209–1213 and 1024–1031 cm^{-1} characterizing the presence of C–O–C stretching vibration in the AS units, clearly demonstrates a rise of the AS unit content in copolymers as AS content changes from 0 to 100%. The IR spectra of all polymers except for EA homopolymer exhibit a sharp peak at 1116–1118 cm^{-1}, which might be due to the in-plane bending vibration of the C–H bond in 1,2,4-trisubstituted phenyl ring. The presence of all these characteristic groups strongly suggests the formation of a real EA/AS copolymer.

3.4. High-resolution ^1H NMR spectra

500 MHz high-resolution ^1H NMR spectra of EA/AS copolymer bases and EA/SA copolymer salts with four EA feed content from 30 to 90 mol%, together with the peak assignments are shown in Figs. 6 and 7 and Table 3. It is seen that the copolymers are characterized by five main signals, corresponding to five types of protons. Both aliphatic and imino protons are easily and accurately assigned, but the aromatic protons are difficult to be exactly assigned because all of the aromatic protons on the two pair of monomer units are similar. However, two series of copolymers exhibit different characteristics of NMR spectra, possibly due to their different polymer forms, i.e. base and salt. For example, the EA/AS copolymer bases exhibit relatively high resolution of the resonance peaks of

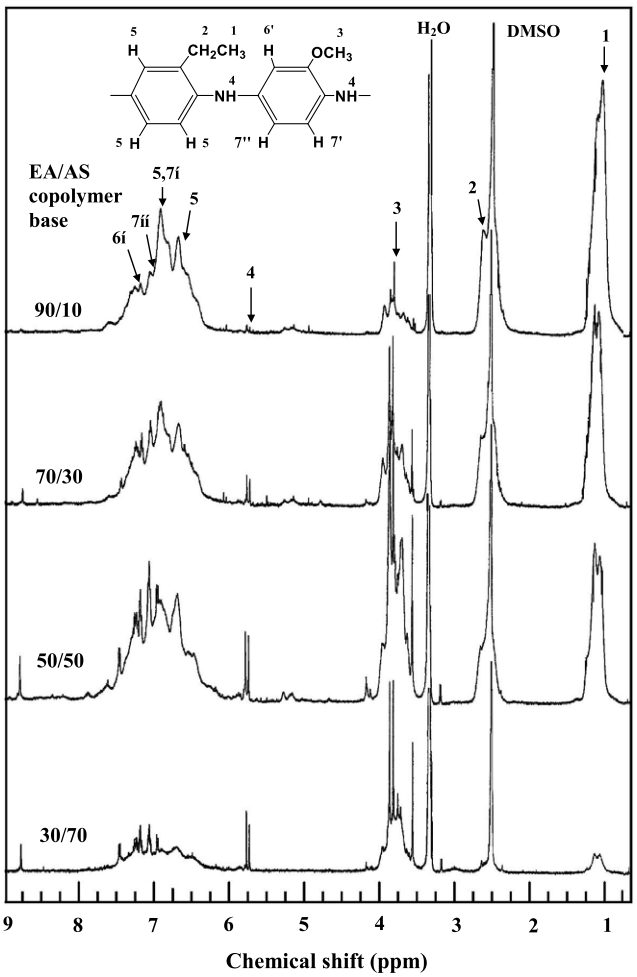

Fig. 6. ^1H NMR spectra of copolymer bases with EA/AS molar ratios of 30/70, 50/50, 70/30, 90/10 in DMSO-d6 at 500 MHz after the scanning number of 64.

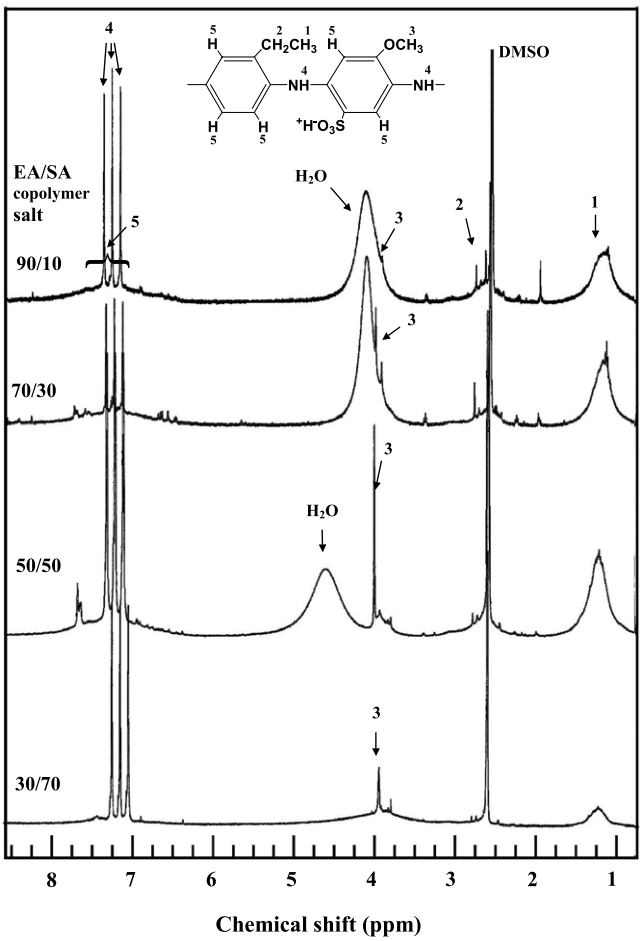

Fig. 7. ^{1}H NMR spectra of copolymer salts with EA/SA molar ratios of 30/70, 50/50, 70/30, 90/10 in DMSO-d6 at 500 MHz after the scanning number of 64.

the aliphatic and aromatic protons but relatively low resolution of the peaks of the imino protons. The situation is almost contrary for the spectra of the EA/SA copolymer salts. In particular, a broad peak from water protons at relatively low field could be owing to a strong interaction between the sulfogroups and water molecules. At higher SA feed content, much stronger interaction between the sulfogroups and water molecules results in significant reduction (at 50 mol% SA) or even disappearance (at 70 mol% SA) of the water proton peak. Furthermore, the EA/SA copolymer salts all exhibit a very sharp triplet of the imino groups (–NH–) [4,5] partly due to their much lower $\bar{M}_n$, as listed in Table 6, while its higher chemical shift should be ascribed to the presence of high electro-negativity of the sulfonic groups. On the contrary, the EA/AS copolymer bases exhibit a very weak and broad peak centered from 5.71 to 5.76 ppm attributed to –NH– linkages. The intensity of the peak corresponding to –NH– group in EA/AS copolymers increases with increasing the AS units, suggesting that the benzenoid structure in the copolymers increases, which is coincided with the results revealed by the IR and UV–vis (Table 4) spectra. Much lower intensity and resolution of the aromatic protons of the EA/SA copolymers are because of the enshrouding effect from much stronger –NH– peaks. No regular variation of the chemical shifts of the protons in the two series of copolymers with comonomer ratio is found, but the chemical shifts of imino and aromatic protons tend to increase with adding the sulfonic groups on the phenyl ring because of their high electro-negativity. These results demonstrate that the EA/AS and EA/SA copolymers were successfully prepared by the chemically oxidative polymerization.

3.5. UV–vis spectra

UV–vis spectra of the EA/AS polymer bases with different comonomer ratios and various oxidant/monomer ratios are compared in detail in Fig. 8. The spectra consist of two major absorption bands, the first absorption band at ~307 nm (4 eV) assigned to $\pi-\pi^*$ transition, and the second band around ~585 nm (2 eV) associated with "exciton" transition. This local change reflected by the exciton transition is sensitive to a chain conformation-related process. The first band shows irregular variation

Table 3
The chemical shifts and possible assignments of high-resolution ^{1}H NMR spectra of EA/AS copolymer emeraldine bases and EA/SA copolymer virgin salts

Monomer feed molar ratio	Aliphatic protons			Imino proton	Aromatic protons		
	1	2	3	4	5, 7′	6, 6′	7, 7″
EA/AS							
90/10	1.05, 1.11	2.50, 2.63	3.68, 3.80, 3.85, 3.92	5.73	6.66, 6.89	7.15, 7.24	7.03
70/30	1.06, 1.13	2.50, 2.64	3.68, 3.80, 3.84, 3.93	5.73, 5.77	6.66, 6.90	7.15, 7.25	7.01
50/50	1.06, 1.13	2.50, 2.64	3.68, 3.80, 3.85, 3.94	5.72, 5.76	6.67, 6.94	7.15, 7.24	7.05
30/70	1.06, 1.13	2.50, 2.65	3.74, 3.80, 3.85, 3.94	5.72, 5.75	6.68, 6.94	7.15, 7.25	7.05
EA/SA							
90/10	1.11	2.50, 2.58	3.88	7.05,7.15,7.25	6.4–8.0		
70/30	1.09	2.50, 2.70	3.84, 3.92	7.03,7.13,7.23	6.3–8.0		
50/50	1.12	2.50, 2.60	3.86, 3.91	7.03,7.14,7.24	6.4–8.0		
30/70	1.17	2.50	3.75, 3.86	6.98,7.09,7.19	6.4–8.0		

The base form of EA/SA (50/50, 30/70) copolymers could not be obtained as a solid powder because of its high solubility in NH_4OH.

Table 4
The ratio of intensity $A(4\text{ eV})/A(2\text{ eV})$ from UV–vis spectra of EA/AS copolymer bases with different molar ratios and oxidant/monomer ratios

EA/AS (Base) in THF	Oxidant/monomer molar ratio	Band I (nm)	Intensity peak $A(4\text{ eV})$	Band II (nm)	Intensity peak $A(2\text{ eV})$	Ratio of intensity $A(4\text{ eV})/A(2\text{ eV})$
100/0	1/2	309	193.2	590	218.8	0.88
90/10	1/2	316	241.9	589	265.4	0.91
70/30	1/2	315	241.3	588	233.9	1.03
50/50	1/2	281	166.6	585	151.5	1.10
30/70	1/2	307	175.3	585	156.5	1.12
30/70	1/3	308	195.7	584	190.6	1.03
30/70	1/2	307	175.3	585	156.5	1.12
30/70	1/1	309	173.0	588	158.8	1.09
30/70	3/2	307	166.9	581	139.2	0.83

while the second band shows a bathochromic shift with increasing EA contents. The bathochromic shift yields a lower energy transition, implying higher stiffness of the molecular chain and thus higher planarity state of the conjugating system. The larger conjugation can be caused by both longer molecular chain and more quinoid units on the molecular chain. It is accord with the fact that the MW analyzed by GPC (Table 1) and the quinoid structures analyzed by FT-IR spectra increase with increasing EA units. From Table 4, it is clearly seen that as the oxidant content increases, the intensity ratio $A(4\text{ eV})/A(2\text{ eV})$ of the two bands decreases, implying that oxidation rate $(1-y)$ increases. According to a principle proposed by Albuquerque et al. [32] to estimate the oxidation state of PAN, in which the $A(4\text{ eV})/A(2\text{ eV})$ ratio declines linearly at a fast rate below $1-y=0.5$ while at a slow rate above this turning point, it could be speculated that the oxidation rate of EA/AS copolymers is above 0.5 owing to a slow reduction of the intensity ratios as the oxidant content increases in Table 4. The band intensity ratio in the EA/AS copolymers also decreases slowly with increasing EA units, indicating more quinoid structures on the molecular chain with an increase in EA content. It again well proves the result of the favorable of quinoid structure in the EA units, just like the results revealed by the IR spectra of the EA/AS copolymers with various compositions.

UV–vis spectra of both emeraldine salt and base of EA/SA polymers with various comonomer ratios are also compared in Fig. 9 and Table 5. It can be seen that the first band of the EA/SA copolymers shows a hypsochromic shift with the increase of SA units. The blue shift of the $\pi-\pi^*$ transition band is in accord with a decreased extent of conjugation caused by an increased phenyl ring torsion angle that results from a steric repulsion between $-SO_3-$ groups and hydrogen on the adjacent phenyl ring. Table 5 demonstrates that the intensity ratio $A(4\text{ eV})/A(2\text{ eV})$ of the EA/SA copolymers increases slowly as the SA content increases, which indicates the oxidation rate of higher than 0.5. It is accorded with the IR analysis of EA/SA copolymers. It can be ascribed to the preferential self-doping with more SA units in the copolymers, whose doping rate is far lower than external doping, making the oxidation rate larger than that with less SA units.

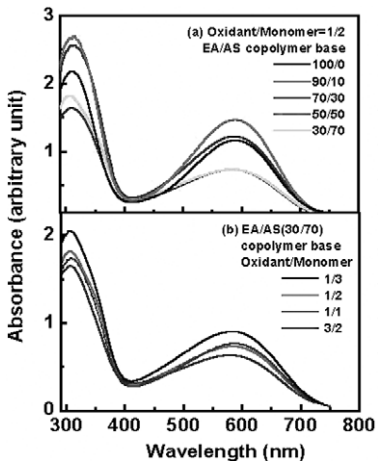

Fig. 8. UV–vis spectra of (a) copolymer bases with EA/AS molar ratios of 100/0, 90/10, 70/30, 50/50, 30/70 in 0.2 mg/ml (THF); (b) EA/AS (30/70) copolymer bases with oxidant/monomer ratios of 1/3, 1/2, 1/1, 3/2 in 0.2 mg/ml (THF).

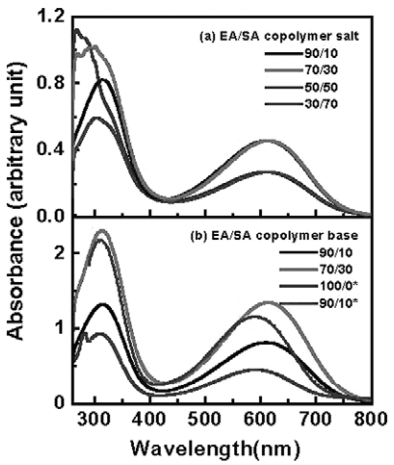

Fig. 9. UV–vis spectra of (a) copolymer salts with EA/SA monomer of 90/10, 70/30, 50/50, 30/70 in 0.17 mg/ml (NMP); (b) copolymer bases with EA/SA monomer ratios 90/10, 70/30 in 0.17 mg/ml (NMP) and EA/SA (Base) $100/0^*$ and $90/10^*$ in 0.17 mg/ml (THF).

Table 5
The intensity ratio A(4 eV)/A(2 eV) from UV–vis spectra of EA/SA copolymers with different molar ratios

EA/SA copolymer in NMP	Polymer form	Band I (nm)	Intensity peaks A(4 eV)	Band II (nm)	Intensity peaks A(2 eV)	Ratio of intensity A(4eV)/A(2eV)
90/10	Virgin salt	315	90.4	610	90.4	1.0
70/30	Virgin salt	297	103.7	607	88.3	1.17
50/50	Virgin salt	283	91.1	613	55.4	1.64
30/70	Virgin salt	303	61.1	613	54.5	1.12
90/10	Base	315	126.4	610	159.1	0.79
70/30	Base	312	221.5	613	257.6	0.86
100/0 (in THF)	Base	309	193.2	590	218.8	0.88
90/10 (in THF)	Base	310	86.6	592	88.7	0.98

3.6. GPC analysis

The MW and its distribution of the copolymer bases of various comonomer ratios and various oxidant/monomer ratios by GPC are listed in Tables 1 and 6. It is easily discovered that as the AS content increases from 0 to 100% both the MW and intrinsic viscosity exhibit a minimal value at AS feed content of 50 mol%, whereas as the SA content increases the MW exhibits a very exquisite reduction. Much lower MW of the EA/SA copolymers than EA/AS copolymers must be attributed to much lower polymerizability of SA monomer than AS monomer, because of much greater steric and electron withdrawing effects of sulfonic groups in SA monomer than AS monomer. With increasing AS or SA contents, the two series of copolymers both exhibit a minimum $\bar{M}_w/\bar{M}_n$. Particularly, EA/AS (50/50) copolymer has the lowest MW whereas EA/AS (70/30) copolymer has the lowest $\bar{M}_w/\bar{M}_n$ of 1.29. So narrow MW distribution might also be a testimony of the formation of the copolymers between EA and AS monomers, otherwise the distribution should be much wider, even a double-peak distribution for the mixture of two homopolymers. It appears that four EA/AS and EA/SA (90/10) copolymers all exhibit much narrower MW distribution but lower MW than EA homopolymer. It is discovered that the molecular structure of EA is relatively favorable for the intermediates to live compared with AS and SA. The electron-donating effect of the ethyl group on the EA makes the transitional oligomers more stable than AS and SA oligomers and enables them to have lifetime enough to propagate. That is to say, the higher MW of the EA homopolymer is attributed to the stable electronic state of EA monomers, which makes it possible for the further propagation of long polymer chains. On the contrary, the AS containing the methoxy group with a conjugation effect with the phenyl ring has much lower oxidation potential to get polymerized, yet the active transitional oligomers are relatively easy to be terminated. Generally the conjugation effect of the substitutes may lead to lower polymerization potential and then favor the initiation of the polymerization, which is associated with a thermodynamic factor. The electron-donating effect of the substitutes favors the propagation of the polymerization leading to higher MW, which is associated with a kinetic factor. Note that unlike the relationship between the yield and comonomer ratio, two series of copolymers both exhibit a minimum $\bar{M}_w/\bar{M}_n$ value at a special comonomer ratio. EA/AS copolymers also exhibit a minimum MW at 50/50 mol%, indicating that the chain propagations between activated EA end group and AS monomer (or between activated AS end group and EA monomer) are passivated each other, i.e. a retardant copolymerization effect between EA (or AS) end group and AS (or EA) monomer. This retardant copolymerization finally results in lower MW than respective homopolymerizations. These clearly suggest a copolymerization effect between EA and AS or SA monomers, i.e. the two series of copolymers prepared are real copolymers rather than blends of the homopolymers. In addition, lower MW of EA/AS copolymers than corresponding homopolymers may be due to more activated centers at the initiation step by the copolymerization effect between EA and AS monomers, something like the results caused by increasing oxidant content.

Table 6
The molecular weights and polydispersity index of EA/SA copolymer bases in THF

EA/SA copolymer bases	Oxidant/monomer molar ratio	$\bar{M}_n$ (g/mol)	$\bar{M}_w$	$\bar{M}_w/\bar{M}_n$
100/0	1/2	5620	150,90	2.68
90/10	1/1	3260	6310	1.93
70/30	1/1	2350	6900	2.90

The oxidant/monomer ratios also have a great effect on the MW and polydispersity of the copolymers. It is found that the EA/AS (30/70) copolymer formed at the oxidant/monomer molar ratio of 1/2 exhibits the highest MW but the lowest $\bar{M}_w/\bar{M}_n$, i.e. the oxidant/monomer ratio of 1/2 seems to be optimal for the EA/AS copolymerization to prepare a high MW copolymer. Same relationship between the MW and oxidant/monomer ratio was found for AN/3-sulfonated AN copolymer [28]. It should be noted that all EA/AS copolymers obtained in this study exhibit substantially higher $\bar{M}_n$ and much narrower MW distribution than other

AN copolymers like AN/3-sulfonated AN copolymer ($\bar{M}_n = 3400$ and $\bar{M}_w/\bar{M}_n = 5.1$) [18] and AN/*o*-aminophenoxy-*n*-propyl(or *n*-butyl)sulfonic acid copolymer ($\bar{M}_n = 1700 - 3500$) [19]. As to the EA/SA copolymers, their much lower $\bar{M}_n$ and wider polydispersity than EA/AS copolymers could be ascribed to the great steric and strong electron-withdrawing effects of the $-SO_3H$ group that leads to more difficult chain propagation.

3.7. Solubility

The solubility of EA/SA copolymers in various solvents with broad characteristics is listed in Table 7. All of the EA/SA copolymer salts and bases exhibit good solubility in the solvents with the solubility parameter of 23–27 $J^{1/2}/cm^{3/2}$, dielectric constant of 12–101, and polarity index of 6.4–7.4. It is also found that as the SA unit content in the copolymers increases, the solubility of the copolymer salts keeps excellent in H_2SO_4, NMP, formic acid, and *m*-cresol, but becomes better in both DMSO and DMF, which is also ascribed to the effect of the sulfonic substitution. Note that most of the EA/SA copolymers exhibit much better solubility than other sulfonic group-containing AN copolymers such as AS or toluidine/*m*-SAN copolymers that are mostly soluble in *m*-cresol and moderately soluble in the solvents such as DMF, DMSO, and NMP [21]. Particularly, the EA/SA copolymers with SA feed content from 50 to 70 mol% are completely soluble in 0.1 M NH_4OH. Therefore, the corresponding EA/SA copolymer bases could not be obtained as solid powders and thus the solubility in the solvents could not be listed in Table 7.

Similar principles of the solvent parameters are also applied to the EA/AS copolymers. The copolymer bases are completely soluble in NMP at the copolymer concentration of at least 8 g/L solvent (Table 1), and substantially soluble in all solvents listed in Table 7 except for toluene and xylene. The copolymer salts also exhibit good solubility in NMP, formic acid, *m*-cresol, DMSO, DMF and concentrated H_2SO_4, but hardly ever soluble in benzene, THF, $CHCl_3$, toluene, and xylene. Note that the EA/AS copolymer salts containing EA feed content of 70–100 mol% exhibit relatively poor solubility in *m*-cresol, DMSO, DMF, possibly due to their higher MW, as listed in Table 1. In addition, the solubility of EA/AS (30/70) copolymer in NMP also becomes better with the variation of the oxidants from $FeCl_3$, $FeCl_3/H_2O_2$, $K_2S_2O_8$, $Na_2S_2O_8$, to $(NH_4)_2S_2O_8$. The order of improving solubility is the same as that of enhancing the yield with changing oxidants. This suggests that $(NH_4)_2S_2O_8$ could be optimal oxidant for the preparation of the EA/AS copolymers with better solubility.

It is also found that the EA/SA copolymer salts show the same good solubility as the EA/AS copolymers in solvents such as NMP, formic acid, *m*-cresol, DMSO, DMF and concentrated H_2SO_4. The solubility of EA/SA (90/10) and (70/30) copolymers in DMF increases significantly as compared with the EA/AS copolymers containing the same monomer ratios, possibly due to a contribution from the sulfonic groups. However, the EA/SA copolymer bases have lower solubility in DMSO, THF, benzene and $CHCl_3$ than the EA/AS copolymer bases with the same monomer ratios, indicating that some doping has occurred in the EA/SA copolymer bases, leading to longer conjugation of the molecular chain and thus poorer solubility.

All of the EA/SA and EA/AS copolymer salts and bases exhibit good solubility in the solvents with the solubility parameter of 23–27 $J^{1/2}/cm^{3/2}$, dielectric constant of 12–101, and polarity index of 6.4–7.4, as also shown in Table 7.

3.8. Film-forming ability

Although the film formability is one of the most important processing abilities for the new polymers, it seems that few reports on the film formability of the sulfonated AN copolymers are found till now. The film-forming ability has been studied with NMP and THF as solvents by a solution casting method. It is found that the

Table 7
Solubility of the virgin salts and emeraldine bases of the EA/SA copolymers

Solvents	Solubility parameter ($J^{1/2}/cm^{3/2}$)	Dielectric constant	Polarity index	Solubility and solution color[a]				
				EA/SA (100/0) salt/base	EA/SA (90/10) salt/base	EA/SA (70/30) salt/base	EA/SA (50/50) salt	EA/SA (30/70) salt
H_2SO_4	–	101	–	S,V/S,V	S,V/S,V	S,V/S,V	S,V	S,V
DMSO	27	47	7.2	PS,B/PS,B	S,B/S,B	S,B/MS,B	MS,B	S,G
Formic acid	25	58	(6.5)[b]	S,G/S,G	S,G/S,G	S,G/S,G	S,G	S,G
DMF	25	38	6.4	SS,B/S,B	PS,G/S,G	PS,B/S,B	PS,B	S,B
NMP	23	32	6.7	S,B/S,B	S,B/S,B	S,B/S,B	S,B	S,B[a]
m-Cresol	23	12	7.4	S,G/S,B	S,G/S,G	S,G/S,G	S,G	MS,G
THF	20	7	4.0	IS/S,B	IS/S,B	IS/PS,G	IS	IS
$CHCl_3$	19	5	4.1	IS/S,B	IS/S,B	IS/PS,G	IS	IS
Benzene	19	2	–	SS,B/S,B	IS/S,B	IS/PS,G	IS	IS

[a] B-blue, G-green, V-violet; IS-insoluble, MS-mainly soluble, PS-partly soluble, S-soluble, SS-slightly soluble.
[b] The datum in the parentheses is an estimated value based on the polarity index of acetic acid.

EA/AS copolymer bases exhibit good film formability. The EA/SA (70/30) and (90/10) copolymer bases in NMP also exhibit good film formability, but the film formability of all the EA/SA copolymer salts in NMP is not good enough although the salts are also completely soluble in NMP. It appears that good solubility does not always mean good film formability. The good film formability of the copolymer bases could be due to higher MW and the formation of a real solution. On the other hand, relatively poor film formability of the EA/SA copolymer salts with the same MW might be due to the fact that we did not obtain their real solution in which single chains distribute uniformly in the solvent, though they appear as a solution to naked eyes. It should be noted that the EA/AS copolymer base films formed thus exhibit strong adhesion to glass, and very bright luster due to very smooth surface without defects. It is interesting that the 9×9 cm^2 films cast on glass look like a mirror. You can see yourself very clearly with the black films. These imply that the films are highly amorphous due to a random copolymerization between EA and AS monomers containing two different side groups. The amorphous structure was further confirmed by the observation of polarizing light microscopy because the films cannot transmit any polarized light as well as by the measurement of wide-angle X-ray diffraction because only a broad diffraction peak was observed in the Bragg angles from 6 to 36°.

3.9. Thermal stability

Thermogravimetric (TG) and derivative TG (DTG) curves of the copolymer salts are shown in Figs. 10 and 11 The kinetic parameters of the thermal degradation of the copolymers were calculated by the Friedman technique using the equation [4–7,33–37]:

$$\ln(\mathrm{d}\alpha/\mathrm{d}t) = \ln Z + n\ln(1-\alpha) - E/RT \quad (1)$$

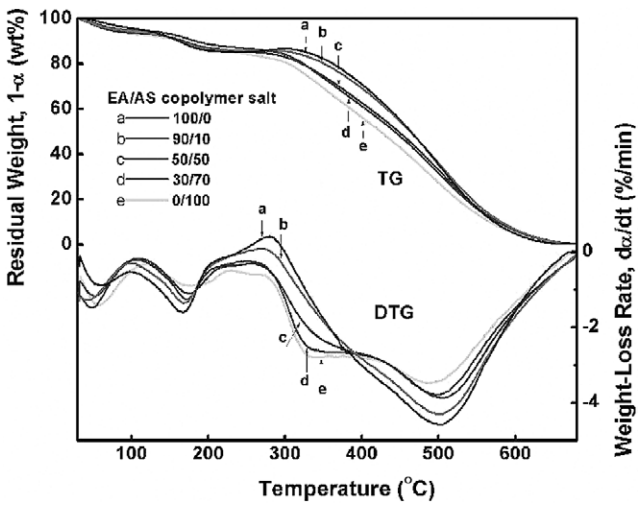

Fig. 10. Thermogravimetry (TG) and derivative thermogravimetry (DTG) of the EA/AS copolymer salts with EA/AS molar ratios of 100/0, 90/10, 50/50, 30/70, and 0/100 at a heating rate of 10 °C/min in static air.

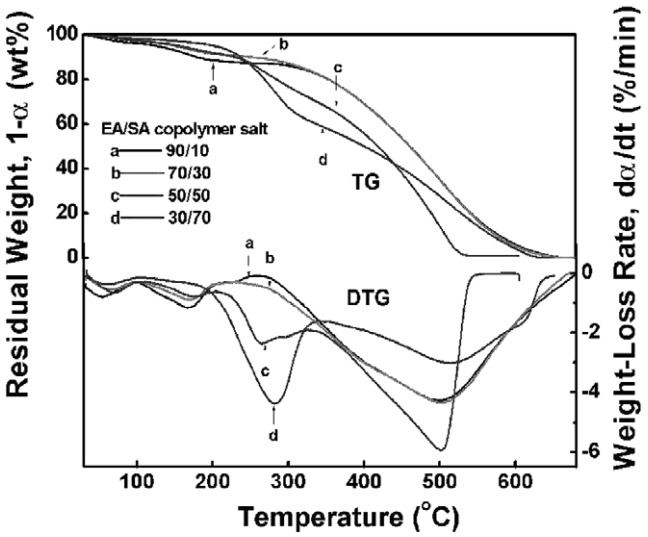

Fig. 11. Thermogravimetry (TG) and derivative thermogravimetry (DTG) of the EA/SA copolymer salts with EA/SA molar ratios of 90/10, 70/30, 50/50, and 30/70 at a heating rate of 10 °C/min in static air.

Where E is activation energy, n decomposition reaction order, and Z frequency Factor. The thermostable and kinetic parameters calculated by Eq. (1) are summarized in Tables 8 and 9. From the DTG curves, two series of copolymers exhibit four major derivative peaks due to the exclusion of water, external dopant (HCl), and methoxy/ethyl/sulfonic (for EA/SA copolymer only) groups, and the thermal / thermo-oxidative degradation of the copolymer backbones, respectively. For the EA/AS copolymers, the peak temperature (T_{HCl}) due to the loss of the HCl increases from 166 to 180 °C with increasing AS content from 0 to 100%, whereas the corresponding maximum weight-loss rate $((\mathrm{d}\alpha/\mathrm{d}t)_{HCl})$ decreases from 1.6 to 0.9 %/min. This implies that the affinity of HCl molecules to the polymer chains becomes stronger with increasing AS content, and the amount of HCl in the copolymers becomes smaller. The initial decomposition temperature (T_d) of the polymer backbones exhibits a minimum at the EA/AS molar ratio of 50/50, probably due to its lowest MW (Table 1). On the contrary, the activation energy, order and frequency factor of the major decomposition exhibit a maximum at the same comonomer ratio of 50/50. The peak temperatures (T_{dm1} and T_{dm2}) to the exclusion of methoxy/ethyl groups and to the thermal/thermo-oxidative decomposition of the polymer backbones, respectively, both decrease from 390 to 339 °C and from 504 to 487 °C as well as the 1st maximum weight-loss rate $((\mathrm{d}\alpha/\mathrm{d}t)_{m1})$ of the polymer backbones increases from 2.3 to 2.8 %/min with increasing AS content from 0 to 100%, but the 2nd maximum weight-loss rate $((\mathrm{d}\alpha/\mathrm{d}t)_{m2})$ of the polymers decreases from 4.6 to 3.5 %/min. This should be attributed to lower thermostability and faster exclusion rate of more methoxy groups-containing copolymers with lower MW (Table 1) than more ethyl groups-containing copolymers. However, the residual char formed after the exclusion of the methoxy groups exhibits a slower decomposition rate

Table 8
The thermal stable parameters of EA/AS copolymer virgin salts with different molar ratios in a static air

EA/AS (mol%)	$T_{HCl}/T_d/T_{dm1}/T_{dm2}$ (°C)	$(d\alpha/dt)_{HCl}/(d\alpha/dt)_{m1}/(d\alpha/dt)_{m2}$ (%/min)	E (kJ/mol)	n	ln Z (min^{-1})
100/0	166/280/390/504	1.6/2.3/4.6	7.65	0.9	7.27
90/10	170/273/380/504	1.3/2.4/4.3	7.72	1.0	7.27
50/50	172/253/370/501	1.2/2.5/3.9	8.23	1.1	7.92
30/70	176/256/343/501	1.1/2.7/3.8	8.04	0.9	7.39
0/100	180/263/339/487	0.9/2.8/3.5	5.71	0.6	5.05

at elevated temperature, leading very broad DTG peaks. Thermal degradation parameters summarized in Table 8 quantitatively provide a deeper insight into the thermal stability and kinetics of the EA/AS copolymers.

For the EA/SA copolymers in Table 9, their decomposition temperatures corresponding to the four derivative peaks are 60 °C (water evaporation), 166–176 °C (T_{HCl}), 231–281 °C (T_{SO3H}) and 501–504 °C (T_{dm}). The assignments of the two higher temperature peaks are further testified by the DTG thermogram of sulfonated PAN, where the peak temperatures due to the SO_3 evolution and backbone degradation are 300–325 and 525 °C, respectively [28,38]. As the SA content increases, the peak temperature (T_{HCl}) increases steadily but the corresponding maximum weight-loss rate ($(d\alpha/dt)_{HCl}$) decreases continuously; both the peak temperature (T_{dm}) and its corresponding maximum weight-loss rate ($(d\alpha/dt)_m$) exhibit a reduced tendency; and the activation energy of the thermal degradation shows a maximum at the EA/SA molar ratio of 50/50. These characteristics are almost the same as those of the EA/AS copolymers. The difference is that the initial decomposition temperature (T_d) of the polymer backbones decreases monotonically with increasing SA content because the copolymers containing more SA units exhibit lower MW. In addition, both the peak temperature (T_{SO3H}) and its corresponding maximum weight-loss rate ($(d\alpha/dt)_{SO3H}$) exhibit an increased tendency with increasing SA content, indicating the exclusion of the $-SO_3H$ groups in the EA/SA copolymers becomes more difficult with increasing $-SO_3H$ groups because of a stronger interaction among the macromolecular chains caused by the $-SO_3H$ groups. Slower maximum exclusion rate of HCl but faster maximum exclusion rate of $-SO_3H$ groups with increasing $-SO_3H$ groups indicate that more SA units lead to less external doping but more self-doping, which is consistent with fluorescence analysis. As indicated in Table 2, the Cl^- anion content decreases dramatically with an increase in sulfonic groups in the copolymers, demonstrating a priority of self-doping in sulfonated AN copolymers in the competition between self-doping and external doping. After a careful comparison of Tables 8 with 9, it is easily found that the incorporation of sulfonic groups decreases the thermostability and delays weight-loss rate at a similar temperature possibly due to much lower MW of the EA/SA copolymers (Table 6). These thermostable results illustrate an easy exclusion of the ethyl, methoxyl, and sulfonic groups on the main chains at elevated temperature. In order to prevent the exclusion of the side groups, the thermal processing temperature of the EA/AS copolymers should be lower than 250 °C, while the processing temperature of the EA/SA copolymers should be lower than 170–250 °C, depending on the EA/SA ratio. The application temperature of the copolymers should be lower than 160 °C in order to avoid the thermal evolution of external dopant HCl, i.e. thermal dedoping.

4. Conclusions

Two series of copolymerizations of EA and AS or SA monomers are successfully carried out in order to prepare uniform copolymer particles, characterize their molecular structure, and improve their solubility, film formability and thermal stability. The homopolymerizing activity of the

Table 9
The thermal stable parameters of EA/SA copolymer virgin salts with different molar ratios in a static air

EA/SA (mol%)	$T_{HCl}/T_d/T_{SO3H}/T_{dm}$ (°C)	$(d\alpha/dt)_{HCl}/(d\alpha/dt)_{SO3H}/(d\alpha/dt)_m$ (%/min)	E (kJ/mol)	n
100/0	166/280/390[a]/504	1.6/2.3[b]/4.6	7.65	0.9
90/10	168/260/231/501	1.2/0.3/4.2	6.40	0.5
70/30	169/228/–/501	0.9/–/4.3	6.43	0.5
50/50	176/206/264/501	0.8/2.3/5.9	9.95	0.9
30/70	–/175/281/501	–/4.3/3.0	7.63	1.2

[a] The temperature at maximum weight-loss rate due to the exclusion of ethyl groups.
[b] The maximum weight-loss rate due to the exclusion of ethyl groups.

three monomers ranks in the order of SA < EA < AS, whereas the copolymerization activity in EA/AS and EA/SA comonomer pairs ranks in the order of EA ≤ SA < AS. The EA monomer is more favorable for the higher MW in both EA/AS and EA/SA copolymers. The electron-donating effect of the ethyl group on the phenyl ring makes it more stable for the transitional oligomers to live, which leads to higher MW. The conjugating effect of methoxy group favors protonation and propagation, resulting in lower oxidation potential and higher polymerization yield. With increasing EA content in the two series of copolymers, the polymerization yield exhibits a maximum but MW and its distribution both exhibit a minimum. The quinoid structures are more favorable on the EA units in the both copolymers and their oxidation states are larger than 0.5. The particle size and its distribution of the EA/SA copolymers exhibit a significant dependency on the polymerization time, comonomer ratio, and alkaline treatment. With increasing SA content or dedoping, both the mean diameter and its standard deviation of the particles decrease steadily down to 218 and 131 nm, respectively, which is related to an increased electrostatic repulsion of negative sulfonic groups on the particle surface of the polymers with spherical chain configuration. Moreover, the particles have existed stably in HCl aqueous solution for at least 6 months, suggesting that SA monomer could be served as an internal stabilizer for the formation and stabilization of the particles. A new simple method of preparing sub-micrometer particles of AN derivative polymers without external stabilizer has been inaugurated. The EA/AS and EA/SA copolymers are completely soluble in many solvents with high solubility parameter, dielectric constant, or polarity index. Two series of copolymer bases exhibit good film-forming ability, and a smooth black film with a bright luster like a mirror and good adhesion to glass has been easily obtained. The thermal stability of the EA/AS and EA/SA copolymer particles is semi-quantitatively correlated with their doping acid, substituent, and MW.

Acknowledgements

The project is supported by (1) the two National Nature Science Foundations of China (20174028 and 20274030); (2) the Foundation of Nano Science Technology Project of Shanghai China(0259nm022); (3) the Foundation of Shanghai Leading Academic Discipline, Donghua University, China; (4) the Key Laboratory of Molecular Engineering of Polymers China. We are grateful to Prof. Dr Yu-Liang Yang and Wei Zhang (Fudan University), and Dr Shou-Ye Yang in the Key Laboratory of Marine Geology, for their valuable helps.

References

[1] Li XG, Huang MR, Duan W, Yang YL. Chem Rev 2002;102:2925.
[2] Halls JJM, Walsh CA, Greenham NC, Marseglia EA, Friend RH, Moratti SC, Holmes AB. Nature 1995;376:498.
[3] Friend RH, Gymer RW, Holmes AB, Burroughes JH, Marks RN, Taliani C, Bradley DDC, Dos Santos DA, Bredas JL, Salaneck WR. Nature 1999;397:121.
[4] Li XG, Huang MR, Yang YL. Polymer 2001;42:4099.
[5] Huang MR, Li XG, Yang YL. Polym Degrad Stabil 2001;71:31.
[6] Huang MR, Li XG, Yang YL, Wang XS, Yan D. J Appl Polym Sci 2001;81:1838.
[7] Li XG, Huang MR, Yang YL. Polym J 2000;32:348.
[8] Sivakumar C, Vasudevan T, Gopalan A, Wen TC. Ind Engng Chem Res 2001;40:40.
[9] Yue J, Epstein AJ. J Am Chem Soc 1990;112:2800.
[10] Shimizu S, Saitoh T, Uzawa M, Yuasa M, Yano K, Maruyama T, Watanabe K. Synth Met 1997;85:1337.
[11] Strounina EV, Kane-Magaire LAP, Wallace GG. Synth Met 1999; 106:129.
[12] Chen SA, Hwang GW. J Am Chem Soc 1994;116:7939.
[13] Chan HSO, Ho PKH, Ng SC, Tan BTG, Tan KL. J Am Chem Soc 1995;117:8517.
[14] Chen SA, Hwang GW. J Am Chem Soc 1995;117:10055.
[15] Yue J, Wang ZH, Cromack KR, Epstein AJ, MacDiarmid AG. J Am Chem Soc 1991;113:2665.
[16] Yue J, Epstein AJ, Zhong Z, Gallagher PK, MacDiarmid AG. Synth Met 1991;41:765.
[17] Yue J, Gordon G, Epstein AJ. Polymer 1992;33:4410.
[18] Mav I, Zigon M, Sebenik A. Synth Met 1999;101:717.
[19] Prevost V, Petit A, Pla F. Synth Met 1999;104:79.
[20] Tang H, Kitani A, Yamashita T, Ito S. Synth Met 1998;96:43.
[21] Roy BC, Gupta MD, Bhoumik L, Ray JK. Synth Met 2002;130:27.
[22] Fan J, Wan M, Zhu D. J Polym Sci Part A Polym Chem 1998;36:3013.
[23] Rao PS, Sathyanarayana DN. J Polym Sci Part A Polym Chem 2002; 40:4065.
[24] Chattopadhyay D, Banerjee S, Chakravorty D, Mandal BM. Langmuir 1998;14:1544.
[25] Min G. Synth Met 2001;119:273.
[26] Qi Z, Pickup PG. Chem Mater 1997;9:2934.
[27] Mattoso LHC, Manohar SK, MacDiarmid AG, Epstein AJ. J Polym Sci Part A Polym Chem 1995;33:1227.
[28] Mav I, Zigon M, Sebenik A, Vohlidal J. J Polym Sci Part A Polym Chem 2000;38:3390.
[29] Choi HJ, Kim JW, Suh MS, Shin MJ, To K. Int J Mod Phys 2001;B15: 649.
[30] Wu Q, Xue Z, Qi Z, Wang F. Synth Met 2000;108:107.
[31] Ishizu K, Honda K. Polymer 1997;38:689.
[32] Albuquerque JE, Mattoso LHC, Balogh DT, Faria RM, Masters JG, MacDiarmid AG. Synth Meth 2000;113:19.
[33] Huang MR, Li XG. J Appl Polym Sci 1998;68:293.
[34] Li XG, Wang LX, Huang MR, Zhu MF, Menner A, Springer J. Polymer 2001;42:6095.
[35] Li XG, Huang MR, Li F, Cai WJ, Jin Z, Yang YL. J Polym Sci Part A Polym Chem 2000;38:4407.
[36] Li XG, Duan W, Huang MR, Yang YL. J Polym Sci Part A Polym Chem 2001;39:3989.
[37] Li XG, Huang MR, Wang LX, Zhu MF, Menner A, Springer J. Synth Met 2001;123:435.
[38] Koul S, Dhawan SK, Chandra R. Synth Met 2001;124:295.